Effect of the Al/O ratio on the Al reaction of aluminized RDX-based explosives

Qian Zhao(赵倩), Jian-Xin Nie(聂建新)†, Wei Zhang(张伟), Qiu-Shi Wang(王秋实), and Qing-Jie Jiao(焦清介)

State Key Laboratory of Explosion Science and Technology, Beijing Institute of Technology, Beijing 100081, *China*

(Received 20 November 2016; revised manuscript received 4 January 2017; published online 6 April 2017)

Aluminum (Al) powders are used in composite explosives as a typical reducing agent for improving explosion performance. To understand energy release of aluminum in aluminized RDX-based explosives, a series of thermal measurements and underwater explosion (UNDEX) experiments were conducted. Lithium fluoride (LiF) was added in RDX-based explosives, as a replacement of aluminum, and used in constant temperature calorimeter experiments and UNDEXs. The influence of aluminum powder on explosion heat (Q_v) was measured. A rich supply of data about aluminum energy release rate was gained. There are other oxides (CO_2, CO, and H_2O) in detonation products besides alumina when the content of RDX is maintained at the same levels. Aluminum cannot fully combine with oxygen in the detonation products. To study the relationship between the explosive formulation and energy release, pressure and impulse signals in underwater experiments were recorded and analyzed after charges were initiated underwater. The shock wave energy (E_{sk}), bubble energy (E_b), and total energy (E_t) monotony increase with the Al/O ratio, while the growth rates of the shock wave energy, bubble energy, and total energy become slow.

Keywords: explosion mechanics, aluminized RDX-based explosive, underwater explosion, explosion heat

PACS: 47.40.–x, 47.40.Rs, 47.70.–n, 47.70.Nd **DOI:** 10.1088/1674-1056/26/5/054502

1. Introduction

The oxidized characteristic of aluminum and detonation products is significant to studies on characteristics of aluminized explosives in the field of energetic materials.[1,2] When aluminum burns in a composite solid propellant, it typically reacts with gas products of the energetic oxidizer and binders, such as H_2O, CO, and CO_2.[3–5] Under some conditions, the addition of aluminum powder can strongly reduce the explosion performance, similar to chemically inert substances such as NaCl, SiO_2, lithium fluoride, and talc.[6] Thus, a displacement with lithium fluoride as an inert salt was studied by Trzcinski and Cookin.[7,8] After that lithium fluoride was used as an inert surrogate for aluminum because it has very similar density and shock impedance and is not expected to participate in detonation and post-detonation expansion.[9]

There are a great number of researchers devoted to finding out exactly how many aluminum powders contribute to the energy release of mixed explosives. Cowperthwaite[10] proposed that approximately 70% of aluminum reacted in detonation reaction zone through a comparison between theoretical calculation and experimental phenomena. Ding[11] studied Hexal PW30 in 1994 and concluded that aluminum powders produced heat release before and after detonation wave front. In 1999, Keicher[12] concluded that up to 30% of the aluminum of non-ideal explosives was completely oxidized without an external oxygen source such as air or surrounding water. According to Waldemar, experimental explosion energy is higher than calculated by CHEETAH with inert aluminum, but it is much lower than the mechanical energy estimated for reactive aluminum.[13] In addition, Ma[14] found that when the Al/O ratio (the atomic ratio of Al and O in the mixed explosive molecular formula) is equal to 0.67, the total energy reached maximum. Ma's article gave no explanation for that phenomenon.

Although preliminary studies showed that the Al/O ratio, the size of aluminum powder, and the morphology of aluminum powders affect the energy release, these studies did not give accurate heat release data from the combustion of aluminum powder in an UNDEX. In the present work, we investigate the effect of the Al/O ratio on the Al energy release rate and the energy release of an underwater explosion (UNDEX). The explosion heat and UNDEX performance of RDX-based aluminized explosives were also measured.

2. Calculation of explosion parameters

In an actual process of explosion, aluminum do not completely react.[15] Therefore, it is important to study relationship between energy release and aluminum reaction. In this study, explosion heat and main explosion products are calculated. Due to a large difference between the experimental results and the calculated results of the maximum heat release principle, the EXPLO5 program is used to calculate the explosion parameters. Two groups of explosive formulation are designed, as shown in Table 1. Sample A is used to get a large scale of the Al/O ratio, from 0 to 1.43. In reality, those proportions (the Al/O ratio > 1) is hard to achieve. Sample B is designed for experimental verification.

†Corresponding author. E-mail: niejx@bit.edu.cn

Table 1. Calculated explosion heat of explosives containing 45% and 52% RDX.

Sample A	Formulation	Al/O	Q_v/MJ·kg^{-1}	Sample B	Formulation	Al/O	Q_v/MJ·kg^{-1}
A1	RDX/binder/Al/LiF 45/8/47/0	1.43	6.97	B1	RDX/binder/Al/LiF 52/8/40/0	1.05	7.80
A2	RDX/binder/Al/LiF 45/8/42/5	1.28	6.93	B2	RDX/binder/Al/LiF 52/8/35/5	0.93	7.74
A3	RDX/binder/Al/LiF 45/8/35/12	1.05	6.88	B3	RDX/binder/Al/LiF 52/8/30/10	0.79	7.70
A4	RDX/binder/Al/LiF 45/8/31/16	0.93	6.86	B4	RDX/binder/Al/LiF 52/8/25/15	0.67	7.62
A5	RDX/binder/Al/LiF 45/8/26/21	0.79	6.84	B5	RDX/binder/Al/LiF 52/8/20/20	0.54	6.67
A6	RDX/binder/Al/LiF 45/8/22/25	0.67	6.63	B6	RDX/binder/Al/LiF 52/8/15/25	0.40	5.81
A7	RDX/binder/Al/LiF 45/8/18/29	0.54	6.06	B7	RDX/binder/Al/LiF 52/8/10/30	0.26	4.80
A8	RDX/binder/Al/LiF 45/8/9/38	0.26	4.22	B8	RDX/binder/Al/LiF 52/8/5/35	0.13	3.88
A9	RDX/binder/Al/LiF 45/8/0/47	0	2.51	B9	RDX/binder/Al/LiF 52/8/0/40	0	2.82

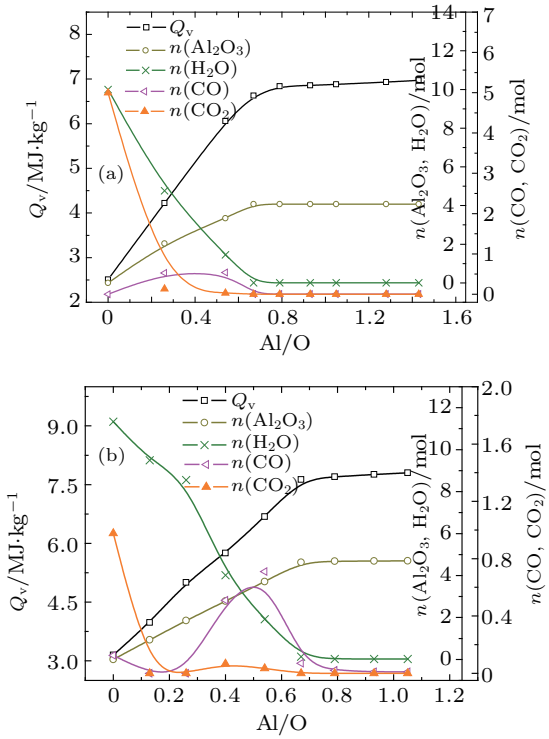

Fig. 1. (color online) Explosion parameters versus Al/O ratio for (a) RDX = 45% and (b) RDX = 52%.

Theoretical calculation results were analyzed and the explosion products were compared one by one. In explosion products, substances with a yield greater than 0.1% are analyzed. As shown in Fig. 1, calculation explosion heat and reaction production of Al_2O_3 increases with the Al/O ratio. The growth rate changes slowly after the Al/O ratio is more than 0.67. The yield of main oxygen-containing products (Al_2O_3, H_2O, CO, and CO_2), reduces monotonously. All of oxygen-containing gases have an inflection point at 0.67. CO_2 runs out and CO has surplus with the amount of aluminum increase. The elemental oxygen in explosion products keeps decreasing when the Al/O ratio increases to 1.43. Elemental oxygen in H_2O, CO_2, and CO is not completely combined with aluminum powder. This is the reason for increasing explosion heat. It can be seen from the comparison between Fig. 1(a) and Fig. 1(b), the growth rate of explosion heat is less than 3% when the Al/O ratio is greater than 0.67. The decreases of H_2O, are less than 4%. Content of carbon bonded with oxygen decreases by more than 10% The results showed that explosion heat and content of Al_2O_3 and H_2O have the same turning point at Al/O=0.67. The incomplete reaction of aluminum and explosion products leads to an incomplete energy release of RDX/Al explosives.

3. Calorimetric heat of aluminized RDX-based explosive

To determine whether there is a fixed Al/O ratio that makes all aluminum powders in mixed explosives completely oxidized, the explosion heats of explosives containing 45% RDX were calculated. Mixtures containing 0, 20%, 25%, 35%, and 40% aluminum content were prepared. The main explosive formulations were two typical RDX-based explosives of aluminum enriched RDX compositions and lithium fluoride enriched RDX compositions. Table 2 shows the formulation and properties of the pouring charges.

Table 2. Formulation and properties of sample charges.

No.	Formulation	Mass ratio	Al/O	ρ_0/g·cm^{-3}
1	RDX/binder/Al/LiF	52:8:40:0	1.05	1.69
2	RDX/binder/Al/LiF	52:8:35:5	0.93	1.68
3	RDX/binder/Al/LiF	52:8:25:15	0.67	1.66
4	RDX/binder/Al/LiF	52:8:20:20	0.54	1.64
5	RDX/binder/Al/LiF	52:8:0:40	0	1.56

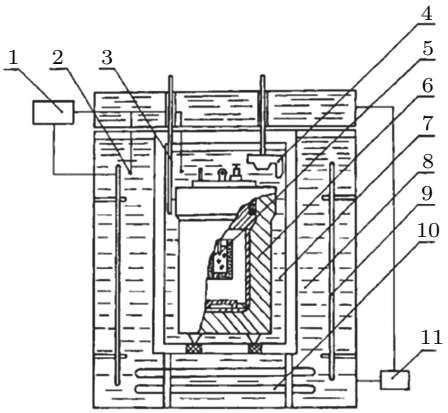

1. temperature control instrument
2. platinum resistance
3. thermometer
4. submersible pump
5. explosive
6. detonation heat bomb
7. hot tub
8. barrel with jacket
9. heating plate
10. cooling snake pipe
11. pump

Fig. 2. Diagram of constant temperature calorimeter.

A measuring device of explosion heat is shown in Fig. 2. The explosion heats were measured in nitrogen environments using a constant temperature calorimeter. An electric detonator with a copper-clad shell was hung below the lid of the calorimeter. The mixed explosive sample (25 ± 0.0002 g) was put into the ceramic shell. It was suspended under the lid of the calorimeter with a silver-plated copper wire. The electric cap was inserted into the sample. Then, the lid was closed and the calorimeter was filled with nitrogen gas. With distilled water as the temperature measuring medium, the outer barrel temperature was adjusted by a temperature control instrument. The temperature of the inner and outer barrel was between 20 and 30 °C. The temperature fluctuation was not more than 0.02 °C in 15 min. At the same time, the temperature difference between the water in the barrel and the outer barrel was not more than 0.03 °C within 15 min. Afterwards, the water temperature in the barrel was recorded. Then, the explosive sample was ignited. About half an hour after the ignition, the water temperature in the barrel was recorded when the change in temperature was less than 0.003 °C in 15 min. Explosion heat was calculated by

$$Q_{\mathrm{vi}} = \frac{C\Delta T - Q_{\mathrm{d}}}{m}, \tag{1}$$

where Q_{vi} is the explosive heat of the explosive specimen at constant volume (J/g), C is the heat capacity of the calorimeter (J/°C), ΔT is the calibrated elevated temperature (°C), and m is the specimen quality (g).

At least two measurements were taken of each formula. The density difference in the two measurements was not greater than 0.02 g/cm^3 and measuring errors were less than 3%. The average values of explosion heat are presented in Table 3.

Table 3. Explosion heat and the energy release degree of each formulation.

No.	Al/O	Q_{vi}/MJ·kg^{-1}	Q_{vcali}/MJ·kg^{-1}	η/%
1	1.05	7.59	7.80	97.23
2	0.93	7.32	7.74	94.26
3	0.67	6.53	7.62	85.70
4	0.54	5.40	6.67	80.96
5	0	2.94	2.98	–

To compare with measured explosion heat, calculation explosion heats are modified. Assuming that the explosion heat is dominated by the energy released by the main explosive component Q_{ve} and the energy released by the combustion of aluminum powder Q_{Al} and Q_{ve} is the value of the modified calculation heat for Al/O = 0. The energy release degree η of aluminum in mixed explosives can be expressed as

$$\eta = \frac{Q_{\mathrm{vi}} - Q_{\mathrm{ve}}}{Q_{\mathrm{vcal}} - Q_{\mathrm{vcale}}} \times 100\%, \tag{2}$$

where Q_{vi} is the explosion heat (MJ/kg), Q_{ve} is the energy released by the main explosive component, Q_{vcal} is thermal heat, and Q_{vcale} is the thermal heat released by the main explosive component.

Lithium fluoride does not take part in the secondary reaction, where the reaction of aluminum powder and detonation products occurs, so the energy release of aluminum can be calculated by subtracting the total energy released by the explosive without aluminum from the total energy provided by all explosive formulations. Because detonation products and aluminum powders are not fully reacted, the energy released in secondary reaction does not reach the theoretical exothermic value in these two cases. As shown in Table 3, a plot of the change in the aluminum energy release rate with the Al/O ratio is shown in Fig. 3. The Al energy release rate increased with increasing Al/O ratio. η reaches 97.81% when the Al/O ratio is equal to 1.05. The explosion heat from theoretical density and actual density are calculated respectively. The calculated data are compared with the measured data. The comparison results are shown in Fig. 4. Thermal heats are basically the same trend at different densities. The measured explosion heat monotonically increases without an inflection point, which is different from calculated data. This is due to the formation of thick oxide layer on the surface of aluminum nucleus in

the process of aluminium oxidation. The active aluminum is prevented from participating in oxidation reaction. Without considering incomplete reaction of active aluminum in interior particle, the main constraint is contents of detonation gas products when the Al/O ratio is more than 0.67 in theoretical calculation. Besides, five aluminized explosives have different initial temperatures. The higher the initial temperature is, the more aluminum powders release energy. Theoretical calculations do not take into account the effect of initial temperature on the energy release rate of aluminum powders.

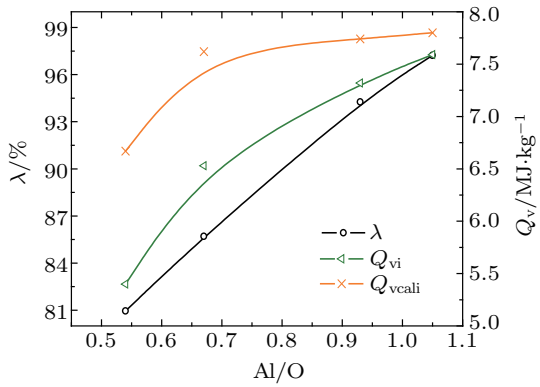

Fig. 3. (color online) Dependence of thermal explosion heat and aluminum energy release rate on the Al/O ratio.

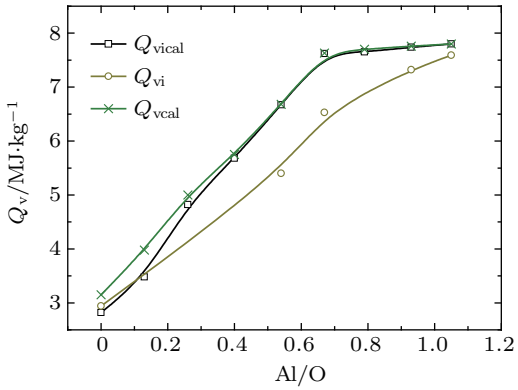

Fig. 4. (color online) Comparison of experimental explosion heat and calculated explosion heat.

Kicinski and Trzcinski[17] used lithium fluoride instead of aluminum and concluded that the aluminum powders are inert in detonation reaction zone. Accordingly, the detonation reaction zone and the secondary reaction zone are completely separated. After RDX detonation, gas products of RDX and metallic substances in mixed explosives are heated to the same temperature. We called the initial temperature (T_0). T_0 is calculated under three basic assumptions: non-equilibrium reaction process in explosion divided into different equilibrium states. Specific heats of compounds in explosive reaction have constant pressure in the aluminum powder combustion stage. The calculation formula of initial temperature is given by

$$Q_v = \Delta H_{mAl} + \Delta H_{mLiF} + \sum_{i=1}^{10} \int_{T_{CJ}}^{T_0} C_{gi} m_{gi} (T_0 - T_{CJ}) \mathrm{d}T + \sum_{j=1}^{2} \int_{T_{CJ}}^{T_0} C_{sj} m_{sj} (T_0 - T_{CJ}) \mathrm{d}T + \sum_{k=1}^{2} \left(\int_{298}^{T_m} C_{sk} m_k (T_m - 298) \mathrm{d}T + \int_{T_m}^{T_0} C_{lk} m_k (T_0 - T_m) \mathrm{d}T \right), \quad (3)$$

$$C = a + bT + cT^2, \quad (4)$$

where ΔH_{mAl} is the fusion enthalpy of aluminum, ΔH_{mLiF} is the fusion enthalpy of lithium fluoride, T_{CJ} is the initial temperature of detonation products. i, j, and k mean the number of gas products, solid products, and metal additives. C_{sj}, C_{ji}, C_{sk}, and C_{lk} mean specific heat at constant pressure of gas products, solid products, solid metal, and liquid metal. m_{gi}, m_{sj}, and m_k mean quality of gas products, solid products, and metal additives.

Equation (4) is the relationship on specific volume and temperature. Thermodynamic parameters and mass of detonation products of pure RDX are shown in Table 4. It also shows the parameters a, b, and c in Eq. (4). Among detonation products only matters with the contents greater than 0.1% in products are listed in Table 4. In the detonation zone, specific heat is usually considered to be constant-volume specific heat due to little volume change. In secondary reaction zone behind detonation wave front, volumetric specific heat capacity is not useful for the gas expansion. Sobaric specific heat capacity is more nearing to reality.

Table 4. The products of RDX and some parameters in Eq. (3) and Eq. (4).

	m/kg	a	b	c
LiF(s)	–	4.18×10^{1}	1.87×10^{-2}	6.94×10^{-7}
LiF(l)	–	6.42×10^{1}	4.20×10^{-14}	-2.30×10^{-17}
C(s,gr)	9.58×10^{-2}	5.39×10^{-1}	9.11×10^{-9}	0.00×10^{0}
H_2O	1.39×10^{-1}	7.76×10^{0}	1.55×10^{-3}	-1.14×10^{-7}
N_2	1.91×10^{-1}	6.77×10^{0}	8.15×10^{-4}	-1.15×10^{-7}
CO_2	1.00×10^{-1}	9.00×10^{0}	3.59×10^{-3}	-8.25×10^{-7}
CO	2.79×10^{-2}	6.79×10^{0}	9.20×10^{-4}	-1.53×10^{-7}
CH_4	1.49×10^{-2}	7.96×10^{0}	7.81×10^{-3}	-1.14×10^{-6}
NH_3	7.19×10^{-3}	2.02×10^{0}	1.98×10^{-3}	-3.61×10^{-7}
CH_2O_2	1.83×10^{-2}	1.17×10^{1}	1.36×10^{-1}	-8.41×10^{-5}
H_2	7.00×10^{-4}	6.92×10^{0}	1.09×10^{-4}	-9.30×10^{-8}
C_2H_6	3.57×10^{-3}	1.64×10^{0}	4.50×10^{-3}	-1.55×10^{-6}
HF	3.00×10^{-4}	2.46×10^{1}	6.89×10^{-3}	-1.24×10^{-6}
Li_2CO_3	1.85×10^{-3}	1.85×10^{2}	-5.10×10^{-8}	3.00×10^{-11}
Al(s)	–	2.81×10^{1}	-5.41×10^{-3}	8.56×10^{-6}
Al(l)	–	3.18×10^{1}	3.94×10^{-11}	-1.79×10^{-14}

Since heat absorption of aluminum powder and lithium fluoride are taken into account, the initial temperature better explains why aluminum energy release rate increased. To analyze the phenomenon of increasing aluminum energy release rate, T_0 and the categories and molar mass of final explosion products were discussed. Among detonation products only the amount of CO_2, CO, and H_2O change with the increase of

Al/O ratio. As displayed in Table 4, the initial temperature increased and the amount of CO_2, CO, and H_2O decreased with increasing Al/O ratio. This illustrates that aluminum powder is more fully combined with elemental oxygen in the product. Meanwhile, the explosion heat and Al energy release rate increase with increasing Al/O ratio.

It is concluded that no matter how much aluminum added, oxygen in detonation products cannot be completely react with aluminum. However, the Al/O ratio increase can continuously improve the energy release degree of explosive by analyzing Figs. 3 and 4 and Table 4.

Table 5. Explosion products in secondary reaction and system initial temperature.

No.	1	2	3	4	5
Al/mol	3.62	1.78	0	0	0
Al_2O_3/mol	4.67	4.67	4.63	3.71	0
CO/mol	5.01×10^{-2}	5.93×10^{-2}	1.27×10^{-1}	1.32	1.00
CO_2/mol	–	–	–	0.05	2.27
H_2O/mol	3.37×10^{-2}	3.75×10^{-2}	7.98×10^{-2}	1.37	7.70
T_0/K	1255.4	1140.3	1109.9	1086.2	1006.4

4. Effect of the Al/O ratio on the property of underwater explosion

In underwater explosion, heat energy and kinetic energy of detonation product gas make the surrounding water vaporization and push the air bubbles expand outwards.[16] Shock wave energy and bubble energy are released in this process. Underwater explosion experiment is carried out on RDX/Al/LiF explosives to study the energy distribution. The main charges were initiated by a nonel blasting cap and a cylindrical pressed JH-14 booster (RDX/ fluororubber and graphite 96.5%:3.5%). In this study, we used two sections of expansion booster. The diameter of the first section booster was 40 mm with a mass of 50 g, and the diameter of the second section booster was 80 mm with a mass of 200 g. The mass of explosive sample is 1 kg. The diameter of explosive columns is 10.0 cm. To investigate the initial reaction time and the energy release degree of metal with the surrounding water medium.

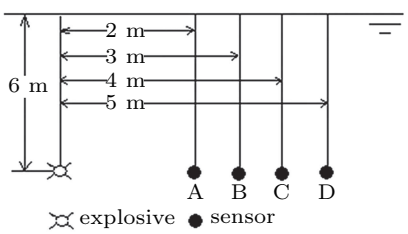

Fig. 5. The UNDEX experiment.

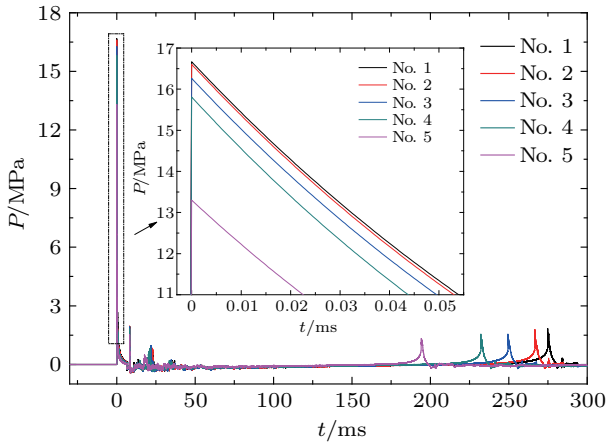

Fig. 6. (color online) Pressure histories with different LiF contents.

As shown in Fig. 5, charges of several formulations were performed in water pool and the pressure time curve was tested and analyzed by pressure transducers (702-QG-W01), and a data collecting instrument (GENESIS 986A0151). For each formulation two identical charges were carried out. Figure 5 shows the scheme of the experimental arrangement. The explosion center and the pressure transducers were at the same level as the horizon and 6 m below the surface of the water. The distances between the explosion center and pressure transducers were 2, 3, 4, and 5 m, respectively. The UNDEX experiments were carried out to discuss the effect of aluminum on energy release. The shock wave histories of composite explosives with different lithium fluoride content were measured and are shown in Fig. 6. It can be seen that the bubble pulsation period and shock wave pressure keep increasing with rising Al/O ratio. However, the change of peak pressure is very small when the Al/O ratio is 0.93. The peak pressure difference between formulation 1 and 2 are very small at the distances of 3, 4, and 5 m. The shock wave energy, bubble energy, total energy, and the volume work (A_0) provided per unit mass of the UNDEX are calculated by[18]

$$E_s = \frac{4\pi R^2}{W\rho C}\int_0^{6.7\theta} P^2(t)\,\mathrm{d}t, \tag{5}$$

$$E_b = K_1 P_H^{5/2} T^3/\rho^{3/2}, \tag{6}$$

$$E_t = \frac{1}{\rho C}(1 - 2.422\times10^{-4}P_m(t) - 1.031\times10^{-8}P_m^2(t))\int_0^{6.7\theta} P^2(t)\,\mathrm{d}t, \tag{7}$$

$$A_0 = K_f(\mu E_{sk} + E_b), \tag{8}$$

$$\mu = 1 + 1.3328\times10^{-1}P_{CJ} - 6.5775\times10^{-3}P_{CJ}^2 + 1.2594\times10^{-4}P_{CJ}^3, \tag{9}$$

where E_{sk} (MJ/kg) is the shock wave energy, E_b (MJ/kg) is the bubble energy, and E_t (MJ/kg) is the total energy in Eqs. (5)–(7). K_e represents the calibration coefficient of a specific shock wave energy, P_H is the hydrostatic pressure at charge, K_1 is the calibration coefficient of a specific bubble energy. W is the explosive quality (kg), ρ is the water density (1.025 g/cm^3), c is

the speed of sound in water (1450 m/s), $P(t)$ is the explosive shock wave pressure (Pa), and T is the bubble pulsation period (s). A_0 is the total specific output energy (MJ·kg^{-1}), μ is a coefficient related to detonation velocity, explosion pressure, and charge density; and K_f is a charge geometry factor. K_f varies between 1.02 and 1.10 for a non-spherical shape. $K_f = 1.02$, given that the tested explosives have a fixed depth-diameter aspect ratio of 1:1. To ensure the sensitivity and accuracy, three initial underwater tests on TNT were done to correct the coefficients, K_e and K_1. The measured the shock energy TNT equivalent and the bubble energy TNT equivalent fitted using theoretical values yielded $K_e = 1.01$ and $K_1 = 3.26 \times 10^2$. The detonator energy and booster energy should be deducted when calculating underwater explosion energy.

Table 6. Energy release of UNDEX.

No.	Al/O	E_{sk}/MJ·kg^{-1}	E_b/MJ·kg^{-1}	E_t/MJ·kg^{-1}	A_0/MJ·kg^{-1}
1	1.05	1.24	4.82	6.06	7.47
2	0.93	1.21	4.45	5.66	7.02
3	0.67	1.07	3.56	4.63	5.82
4	0.54	0.93	2.83	3.76	4.78
5	0	0.55	1.50	2.05	2.64

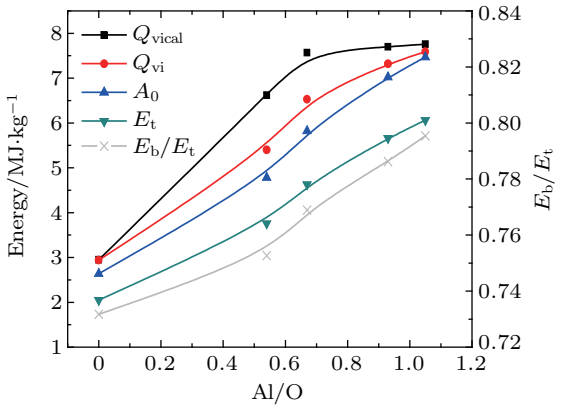

Fig. 7. (color online) Comparison of explosion heat, volume work, and the energy ratio.

Table 6 shows energy parameters of UNDEX for different formulations. The calculated data are average values of results of two duplicate tests at distances of 3, 4, and 5 m, and the difference between duplicate test results is less than 2%. The total energy does not include heat loss which was used to heat the surrounding water. Figure 7 demonstrates explosion heat, volume work, total energy and ratio of bubble energy and total energy. The changing trend of volume work and total energy are consistent with calculated and measured explosion heat. Bubble energy proportion increases with the increase of Al/O ratio in the total energy. The secondary reaction heat produced by aluminum powder combustion mainly increases the bubble energy in UNDEX.

5. Conclusion

To explore the Al reaction and effect of aluminum powder on explosion heat and energy output of UNDEXs, the experimental explosion heats were measured using Al/LiF-containing explosives. The most significant conclusions in the reported experiments are as follows.

(i) Theoretical calculation shows that explosion heat increases monotonously with the Al/O ratio increase. Alumina in explosion products increases. The content of oxygen bonded with carbon and H_2O decreases. The increases of explosion heat and the alumina output begin to slow down when Al/O ratio is greater than 0.67. Contents of H_2O, CO, CO_2 continues to slowly decrease but is still remaining.

(ii) Calorimetric heat measurement experiments confirmed that the increase of explosion heat is monotonic. However it has no turning point at Al/O ratio is 0.67, which is different from the theoretical calculation results. Theoretical calculation results and actual measured results of explosion heat are converging. This illustrates the energy release degree increases along with the Al/O ratio.

(iii) This is the first UNDEX experiment in which the donor explosive content remained unchanged while the amount of aluminum increased. The UNDEX experiment shows that the changing trend of volume work and total energy are consistent with calculated and measured explosion heat. The shock wave energy, bubble energy and total energy increase with the increase of the Al/O ratio when the main explosive content is constant, while the growth rate of the shock wave energy, bubble energy and total energy. The proportion of bubble energy increases in total energy. That means more energy produced by aluminum reaction is used to increase the bubble energy.

References

[1] Yan Z X 2011 *Acta Phys. Sin.* **60** 076202 (in Chinese)
[2] Lin W, Zhou J, Fan X H and Lin Z Y 2015 *Chin. Phys. B* **24** 014701
[3] Beckstead M W, Liang Y and Pudduppakkam K V 2005 *Combust. Explos. Shock.* **41** 533
[4] Brooks K P and Beckstead M W 1995 *J. Propul. Power* **11** 769
[5] Guo F, Zhang H, Hu H Q and Cheng X L 2013 *Chin. Phys. B* **23** 046501
[6] Orlenko L P 2004 *Physics of Explosion* (Moscow: Nauka) p. 235
[7] Trzcinski W A, Cudzilo S, Paszula J and Callaway J 2008 *Propellants Explos. Pyrotech.* **33** 227
[8] Cook M A, Filler A S, Keyes R T, Partridge W S and Ursenbach W O 1957 *J. Phys. Chem.* **61** 189
[9] Manner V W, Pemberton S J, Gunderson J A, Herrera T J, Lloyd J M, Salazar P J, Rae P and Tappan B C 2012 *Propellants Explos. Pyrotech.* **37** 198
[10] Tarver C M, Fried L E, Ruggerio A J and Calef D F 1993 10*th Symposium (International) on Detonation*, July 12–16, 1993, Massachusetts, America, p. 862
[11] Ding G Y and Xu G G 1994 *Acta Armamentarii* **4** 25
[12] Keicher T, Happ A and Kretschmer A 1999 *Propellants Explos. Pyrotech.* **24** 140
[13] Trzcinski W A, Cudzíło S and Szymanczyk L 2007 *Propellants Explos. Pyrotech.* **32** 392
[14] Lin M J, Ma H H, Shen Z W and Wan X Z 2014 *Propellants Explos. Pyrotech.* **39** 230
[15] Zhou Z Q, Nie J X, Guo X Y, Wang Q S, Ou Z C and Jiao Q J 2015 *Chin. Phys. Lett.* **32** 016401
[16] Wang S S, Li M and Ma F 2014 *Acta Phys. Sin.* **63** 194703 (in Chinese)
[17] Kicinski W and Trzcinski W A 2009 *J. Therm Anal. Calorim.* **96** 623
[18] Cole P 1948 *Underwater Explosion* (Princeton: Princeton University Press) p. 502